

Optimization of boriding process on AISI 1015 steel using response surface methodology

Surya Raj Gopala Krishnan¹, Prince Muthiah², Maniraj Jagathan³

¹Anna University, Park College of Engineering and Technology, Department of Mechatronics Engineering, Coimbatore, Tamilnadu, India.

²Anna University, Solamalai College of Engineering, Department of Mechanical Engineering, Madurai, Tamilnadu, India.

³Anna University, Kalaignarkaranidhi Institute of Technology, Department of Mechanical Engineering, Coimbatore, Tamilnadu, India.

e-mail: surya.raj437@gmail.com, drprince1977@gmail.com, maniraj_j@rediffmail.com

ABSTRACT

The goal of this study is to increase the impact toughness of the borided steel without much compromising the surface microhardness. An optimization technique known as Response Surface Methodology was employed to achieve the goal of this work. The pack borided specimens at optimized conditions were analyzed in terms of microstructure, microhardness, XRD, and Impact toughness and compared with borided specimens treated for 950°C for 180minutes. The poly-phase iron borides zone, transition zone, and base metal were all evident. In the iron borides zone, the microhardness was 1745HV, then 345HV in the transition zone, and lastly 245HV in the matrix area. The XRD technique was used to identify the growth of Fe₂B and FeB phases. The impact toughness was 44.182 J when the specimens treated at optimized conditions.

Keywords: Steel; Boriding; Toughness; Optimization; Hardness; Microstructure.

1. INTRODUCTION

Steel is a very influential substance that is widely used in the construction of buildings and dams, manufacturing industries, military and aerospace applications [1]. Despite its high industrialization, this material has a number of issues, including low wear and corrosion resistance [2]. Boriding is an important aspect in overcoming such challenges. Boronizing creates a hard coating layer on the surface, but does not change the interior of the substrate. Thus, the surface resists plastic deformation thanks to its hardness against abrasive environments, while the ductile matrix absorbs the incoming impacts [3]. In general, pack boriding provides exceptionally high surface hardness at a maximum of 2100HV, which is superior than carburizing [4], plasma nitriding [5], and chromizing treatments [6]. It is a more cost-effective and ecologically beneficial approach, not only because it delivers high hardness, but also when compared to other boriding procedures [7]. The pack boriding process is carried out at temperatures ranging from 850°C to 1050°C for 2 to 6 hours [8]. Boron atoms are diffused into the surface region and form a hard iron boride layer during the pack boriding process [9]. In the surface region, this process results in the development of a two-phase iron boride layer, namely FeB and Fe₂B [10]. Boride needles produced a non-homogeneous and acicular structure during this procedure [11]. It is heavily influenced by time, temperature, and chemical composition [12]. It has a low coefficient of friction and is resistant to wear, corrosion, and oxidation [13]. While this technique offers several benefits, it lowers ductility, strength, and toughness [14]. This is related to the brittleness effect. The development of the FeB phase causes extreme brittleness [15]. The thermal expansion numbers of FeB and Fe₂B layers are distinct causing brittleness and pull-off in the coating layers [16]. Many techniques were attempted to overcome this problem, such as interrupted boriding, superplastic boriding, and many multi-component treatments, but none of them have used the multi objective optimization technique (Response Surface Methodology) to find the better toughness value without significantly compromising the value of microhardness.

Despite this, various material handling equipment (drill bits) and machinery parts (gears, crankshafts, train wheels, etc.) are in great demand to fulfill the need for high hardness and high toughness [17, 18]. As a result, several researchers have concentrated on improving mechanical characteristics [19] and tribo properties [20, 21]. Nevertheless, many studies have explored the impact of multicomponent boride layer, but they are unable to maximize the toughness without significantly reducing the microhardness. Many approaches

were available to improve the toughness of the material. Plamqvist, Berkovich, micro indentation, and nano indentation are some ways for measuring the material’s fracture toughness [22, 23].

The probable path for future development of this technique is to improve toughness without significantly compromising hardness while improving toughness of the boride layer.

The objective of this work is to identify the optimum temperature and time in the pack boriding process using response surface methodology in order to improve the toughness without much drop in surface hardness.

2. MATERIALS AND METHODS

2.1. Base material

The fundamental material in this work was commercially available AISI 1015 low carbon steel. A spectrometer was used to determine the chemical composition of this steel sample. Table 1 shows the chemical composition of base material. The cylindrical steel specimens of dimensions 25 mm in diameter and 12.5 mm in height were used. Investigations were conducted using these samples. The samples were properly prepared for metallography in accordance with standards.

2.2. Pack boriding process

The AISI 1015 steel specimens along with pack chemicals (5% B₄C + 5%KBF₄ + 90%SiC) were enclosed in a stainless-steel box. The box was loaded in the muffle furnace. The process time, and the temperature were chosen as a most influencing variables for optimization studies. The process time was varied from 60minutes to 180minutes. The temperature range was 850°C to 1050°C. The schematic of pack boriding process setup is shown in Figure 1.

2.3. Response surface methodology

RSM is one of the reliable statistical and mathematical methods that has been used to model, analyze, and anticipate the right appropriate value for the issues [24]. This method’s goal is to maximize the response (the output variables) in relation to several independent factors (the input variable) [25]. When it is expected that all unreliable variables are measured with minimal error. The most basic model that may be applied in RSM is one that is based on a linear function and the corresponding equation (1) is mentioned below:

$$y = f(x_1, x_2, x_3, \dots, x_i) \tag{1}$$

Where x_i is the number of independent variables and y is the dependent variable.

Table 1: AISI 1015 steel chemical composition (in weight%).

CARBON	SILICON	MANGANESE	PHOSPHORUS	SULPHUR	IRON
0.152	0.246	0.689	0.017	0.001	Balance

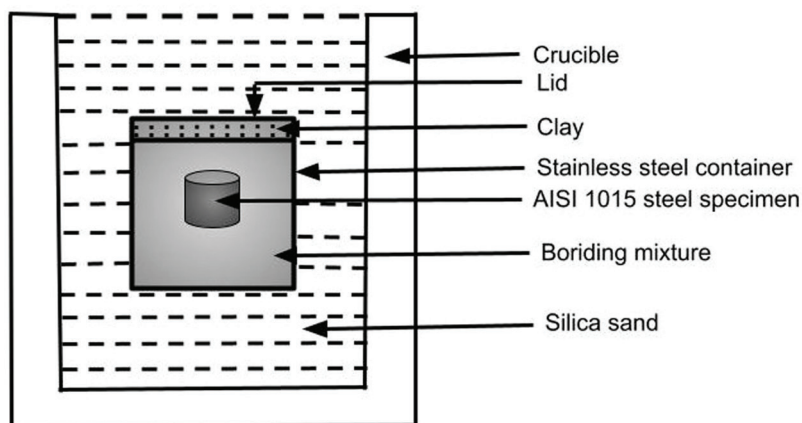


Figure 1: Schematic of pack boriding process setup.

Regression modeling illustrates the relationship between input and output parameters. Analysis of Variance (ANOVA) approach was used to assess the significance of the created model [25]. Utilizing Design-Expert software, three level three factorial designs were conducted in this approach (version 11.5). The central composite design (CCD) approach was used for model development in RSM to analyze the interaction effect on microhardness and toughness of the borided specimen for multivariable (time and temperature) conditions. The goal of applying CCD to the variables used in the present investigation is that the 2nd order model can be developed efficiently [26]. The extra central and axial points in CCD systems allow for the estimation of control parameters in a second-order model. Table 2 shows the list of parameters for pack boriding process. Time and temperature were chosen as the influencing parameters. The minimum (low) and maximum values (high) of time and temperature are mentioned in the Table 2. Using the created regression model, the ideal parameter value for this parameter was obtained. Using numerical approach, optimized parameters were determined.

It is almost hard to detect and manage the minor contributions from each variable, which may have a significant impact on the behavior of the system. As a result, the factors having the greatest influence must be chosen. Screening designs should be used to discover which of the various experimental variables and their interactions have the most significant impacts. Due to their effectiveness and affordability, factorial designs may be used to achieve this goal. Based on the central composite design (CCD), the input and output variables are produced. Thirteen runs were generated according to the CCD. With regard to the state of the input variable, all values for the output parameter are empirically tested. The response data of the pack boriding process is given in Table 3.

2.4. Microstructural analysis

In order to conduct metallographic examinations, the processed specimens were sliced perpendicular to the treated surface. Using emery paper with a 1200 grid, the sample surfaces were polished to a very fine shine.

Table 2: List of pack boriding process parameters for optimization.

NAME	UNITS	LOW	HIGH
Time	Minutes	60	180
Temperature	Celsius	850	1050

Table 3: Response table of pack boriding process.

STD	RUN	FACTOR 1	FACTOR 2	RESPONSE 1	RESPONSE 2
		A:TIME	B:TEMPERATURE	AVERAGE MICROHARDNESS	AVERAGE TOUGHNESS
		MINUTES	CELSIUS	HV	J
3	1	60	1050	1725 ± 17	15 ± 4
11	2	120	950	1785 ± 23	35 ± 5
1	3	60	850	1635 ± 20	45 ± 3
7	4	120	808	1680 ± 22	38 ± 7
5	5	35	950	1610 ± 15	36 ± 6
4	6	180	1050	2150 ± 15	10 ± 3
13	7	120	950	1795 ± 22	31 ± 7
6	8	204	950	1910 ± 25	16 ± 4
10	9	120	950	1825 ± 21	32 ± 5
2	10	180	850	1740 ± 18	28 ± 6
8	11	120	1091	2050 ± 10	12 ± 3
9	12	120	950	1825 ± 22	34 ± 5
12	13	120	950	1810 ± 23	35 ± 6

3% Nital was used to etch the polished specimens' cross sections for 10 seconds to 15 seconds while they were held in atmospheric air. Using a Dwinter optical microscope, the microstructures of pack borided were obtained at the proper magnifications.

2.5. XRD analysis

The phase analyses of borided specimens treated at optimum parameters were examined using XRD (SHIMADZU) at 30 mA and 30 kV with CoK radiation with $\lambda = 1.78897 \text{ \AA}$. The scanning speed and range are set at $5^\circ/\text{min}$ and $10\text{--}80^\circ$, respectively.

2.6. Microhardness analysis

Vickers Mitutoyo microhardness tester was used to quantify microhardness in accordance with ASTM E384 standards from the surface to the core. This study made use of a 50 g load. For the borided specimens, the hardness change throughout the depth was investigated. The value of microhardness was measured at five different locations and the average value was taken in an account and mentioned in Table 3.

2.7. Impact analysis

Using a Charpy impact testing equipment, impact tests were performed. The material utilized for this test has the following measurements: 55 mm length, 10 mm width, and 10 mm thickness. The V-shaped notch had dimensions of 2 mm in width and depth and a 45° angle respectively. The Charpy impact toughness in joules was evaluated for the pack-borided specimens. This test was carried for three times and the average value of Impact toughness was noted and mentioned in Table 3. Scanning electron microscopy was used to analyse the fractured surface.

3. RESULT AND DISCUSSION

3.1. Process parameter optimization

For borided samples, the output responses for micro hardness and toughness were seen in Table 3 for various input values (temperature and time). Thirteen tests had been completed in accordance with the matrix of the two factor, two level central composite design [27].

3.1.1. ANOVA for microhardness and toughness

The main purpose of ANOVA is to analyse the significant parameter and to steer the design space. The results of ANOVA of microhardness and toughness are mentioned in the Tables 4 and 5. If the P value is less than

Table 4: ANOVA for microhardness analysis.

SOURCE	SUM OF SQUARES	DOF	MEAN SQUARE	F-VALUE	p-VALUE	
Model	2.814E+05	5	56279.43	143.51	<0.0001	significant
A-Time	1.138E+05	1	1.138E+05	290.26	<0.0001	
B-Temperature	1.309E+05	1	1.309E+05	333.75	<0.0001	
AB – Time*Temperature	25600.00	1	25600.00	65.28	<0.0001	
A ² – (Time) ²	4006.96	1	4006.96	10.22	0.0151	
B ² – (Temperature) ²	5650.43	1	5650.43	14.41	0.0068	
Residual	2745.13	7	392.16			
Lack of Fit	1465.13	3	488.38	1.53	0.3374	not significant
Pure Error	1280.00	4	320.00			
Cor Total	2.841E+05	12				
Std. Dev.	19.80	R ²	0.9903			
Mean	1810.77	Adjusted R ²	0.9834			
C.V.%	1.09	Predicted R ²	0.9563			
		Adequate Precision	40.7612			

Table 5: ANOVA for Impact toughness analysis.

SOURCE	SUM OF SQUARES	DOF	MEAN SQUARE	F-VALUE	p-VALUE	
Model	1468.41	5	293.68	57.26	<0.0001	significant
A-Time	316.06	1	316.06	61.62	0.0001	
B-Temperature	898.23	1	898.23	175.13	<0.0001	
AB – Time*Temperature	36.00	1	36.00	7.02	0.0330	
A ² – (Time) ²	108.54	1	108.54	21.16	0.0025	
B ² – (Temperature) ²	137.76	1	137.76	26.86	0.0013	
Residual	35.90	7	5.13			
Lack of Fit	22.70	3	7.57	2.29	0.2199	not significant
Pure Error	13.20	4	3.30			
Cor Total	1504.31	12				
Std. Dev.	2.26	R ²	0.9761			
Mean	28.23	Adjusted R ²	0.9591			
C.V.%	8.02	Predicted R ²	0.8790			
		Adequate Precision	22.9871			

0.5 and the F value is greater than 1, the corresponding parameter are considered to be significant [28]. The microhardness model of P value is less than 0.5. Hence, the model is considered to be statistically significant. The model F value of microhardness and toughness are 86.59 and 17.83 which is greater than the value of 1. Hence, the F-value of microhardness and toughness are significant. The R² value is desired as 1, which tends the corresponding model to be significant. The R² value for microhardness and toughness are 0.9841 and 0.9272 respectively. Adequate Precision measures the signal to noise ratio [29]. A ratio greater than 4 is desirable. 31.5050 and 13.1415 are the adequated precision values obtained for microhardness and toughness which indicates the value is greater than 4. So the corresponding values are statically significant.

The unexpected variability in the data is determined by the coefficient of variant (C.V.) [30]. The observed C.V. values for microhardness, and toughness are 1.09%, and 8.02%, respectively. These trials should have adequate reliability and accuracy, according to their low C.V. [31]. The lack of fit (LOF) compares the residual error from the repeated experimental design points to the pure error. Microhardness and toughness all have LOF values larger than 0.05, indicating that the LOF of these models is negligible [32]. The findings of the ANOVA test in Tables 4 and 5 indicate that the Temperature (B) and Time (A) are both expected to be important influencing factors. The microhardness, and toughness are not significantly impacted by the interaction (AB) effect or second order effects of A² and B².

The statistical findings from ANOVA (Tables 4 and 5) supported the relevance of temperature. The p-values for microhardness and toughness are 0.0001, and 0.0001, respectively, which are fewer than the p-values mentioned for time. As a result, the temperature as well as time has the most influential parameters in this model for controlling the responses. The regression model in the form of actual variables may be written as follows:

$$\text{Microhardness} = +4350.43890 - 9.07862A - 5.73593B + 0.013333AB - 0.006667A^2 + 0.002850B^2 \quad (2)$$

$$\text{Toughness} = -213.77759 - 0.316426A + 0.679538B + 0.005AB - 0.001097A^2 - 0.000445B^2 \quad (3)$$

$$\text{Microhardness} = +1808.00 + 119.28A + 127.91B + 80.00AB - 24.00A^2 + 28.50B^2 \quad (4)$$

$$\text{Toughness} = +33.40 - 6.29A - 10.60B + 3.00AB - 3.95A^2 - 4.45B^2 \quad (5)$$

The interaction effect and behaviour of the microhardness and toughness for the chosen two input parameters are shown using the 2D contour and 3D surface graphs (shown in Figure 2). Figure 2(a) and (b) illustrate the connection between time and temperature and the hardness of the boron layer. Increasing the

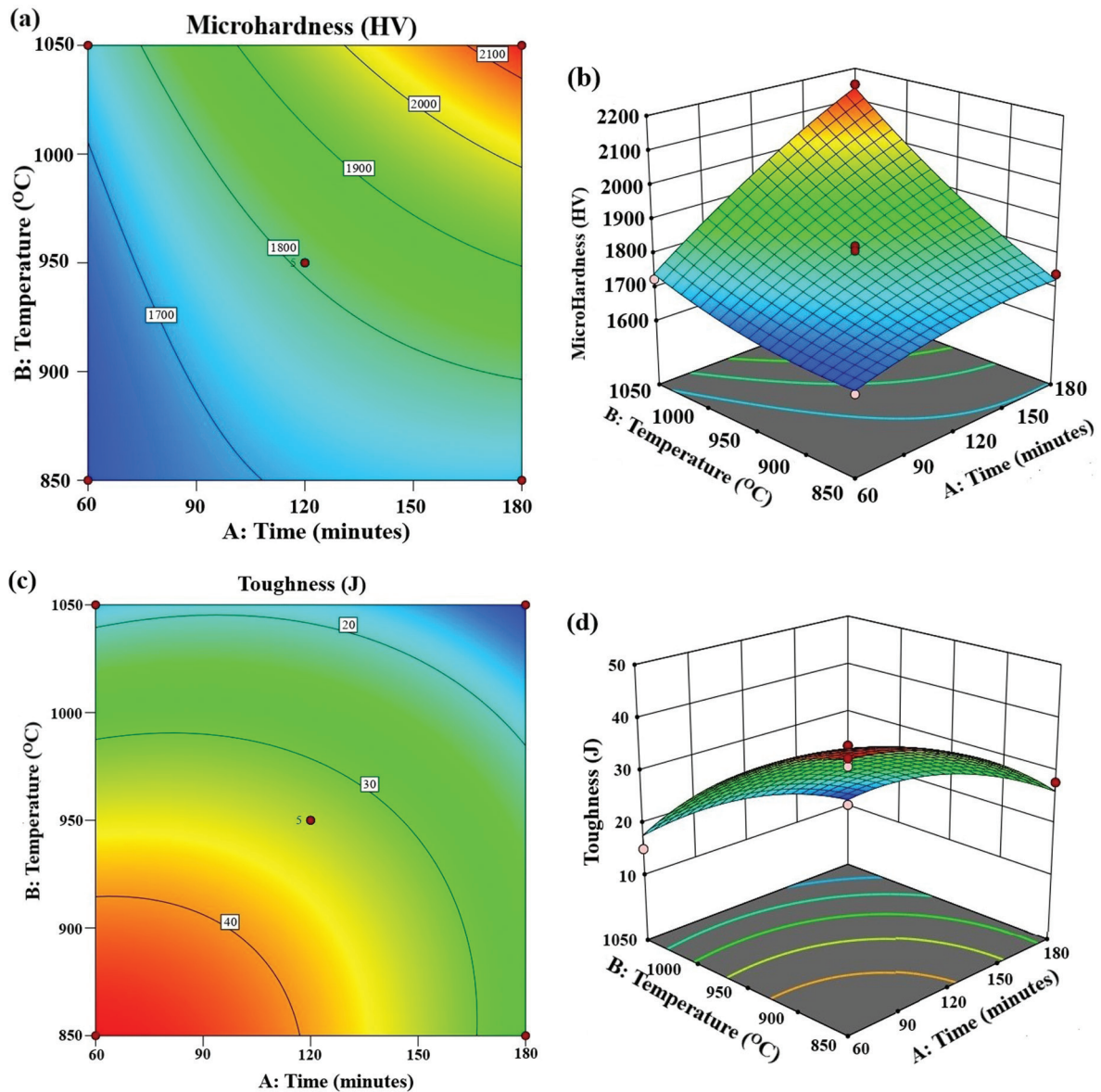


Figure 2: (a, c) 2D and 3D plots of pack borided at 850°C 60minutes and (b, d) pack borided at 950°C 180minutes.

temperature and prolongation period above 950°C will increase the hardness to its maximum. The contour and surface plots in Figure 2(c) and (d), respectively, illustrate the interaction impact of time and temperature on the toughness. The response surface plot showed that, when compared to 850°C temperature with low duration of time had more improvement to the value of toughness. At high temperature and long duration of time leads to poor toughness value due to the parameter of high brittleness.

3.2. Numerical analysis

3.2.1. Desirability approach

Finding the ideal boriding process settings may be difficult due to the large number of quadratic and interaction terms with independent factors. To solve this issue, the combined objective optimization method should be employed. Finding the independent conditions on the variables that drive the output variables to their ideal levels is the aim of multi-objective optimization. The goal in this case is to identify the ideal set of settings that satisfy several objectives, compromising microhardness, and higher toughness. A numerical strategy for solving a mixed objective optimization issue is the desirability function [25]. Between 0 and 1 is desirable. The desirability value 1 reflects the ideal configuration for the chosen response, whereas the desirability value 0 denotes an unsatisfactory design.

Table 6 shows the optimization criteria (goals and factor range) for this optimization model. Except for hardness, which is specified in range, all parameters are given equal priority during the optimization process. The best values should meet the aims of maximizing toughness and ranged microhardness. Table 8 displays the solutions achieved for the specified range and criteria. The contour plot for overall desirability is presented in Figure 3, which depicts the desire for the optimized boronizing settings with a combined desirability rating of 0.989. The optimized values are shown in Figure 3 and the data are represented in Table 7. The best pack boronizing process parameters are microhardness 1656HV and 44 J toughness.

To plan the experiment, the RSM method is used. The results of the values predicted by both responses are found, and the optimization strategy suggests the best process parameters. During the execution of the operation, it is typical to discover the discrepancy between the real and projected value.

Table 6: Goals and factors of pack boriding process.

NAME	GOAL	LOWER LIMIT	UPPER LIMIT	LOWER WEIGHT	UPPER WEIGHT	IMPORTANCE
A-Time	minimize	60	180	1	1	3
B-Temperature	minimize	850	1050	1	1	3
Microhardness	is in range	1610	2150	1	1	4
Toughness'	maximize	10	40	1	1	5

Table 7: Solutions table of boriding process.

NUMBER	TIME	TEMPERATURE	MICROHARDNESS	IMPACT TOUGHNESS	DESIRABILITY	
1	62.668	850.000	1649.143	44.812	0.989	selected
2	73.487	850.000	1670.700	40.930	0.968	
3	67.922	850.000	1656.415	44.630	0.966	
4	81.457	850.001	1683.733	40.677	0.948	

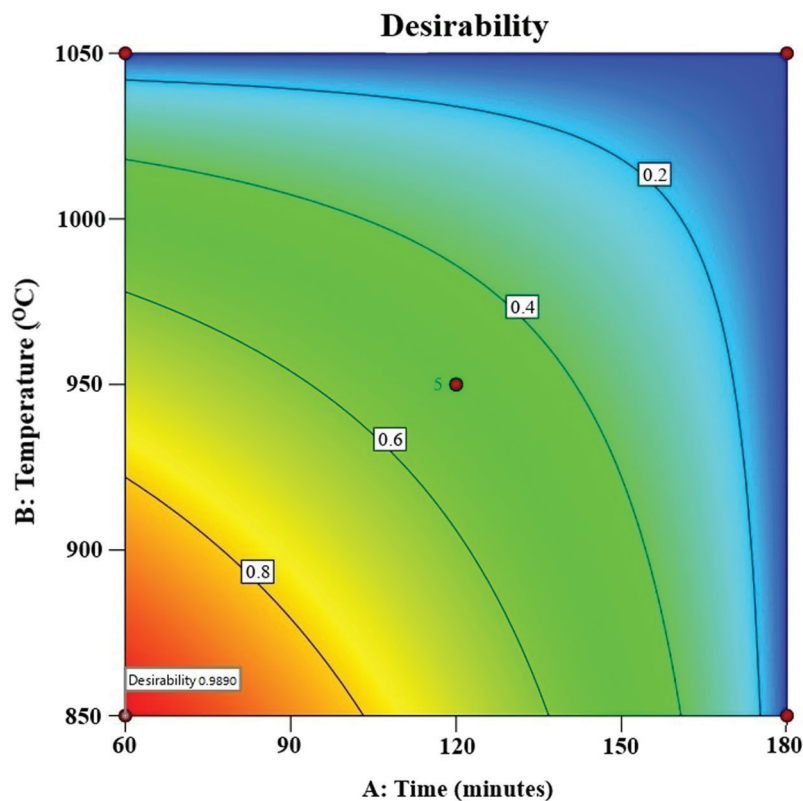


Figure 3: Desirability approach for optimized pack boriding process parameters.

3.2.2. Validation result

The proportion of error is calculated by comparing the expected and actual results in the validation test. The validation tests for the relevant parameter are shown in Table 8. The difference in error between experimental and anticipated values is less than 4.5%, which is acceptable. The validation result shows that there is high agreement between experimental and predicted values. As a result, the RSM-derived optimum parameter offers better accuracy.

3.3. Microstructural analysis

The microstructure of pack borided specimen are shown in Figure 4. It exhibits three different zones 1. Iron borided zone 2. Transition zone and 3. Base metal. The optimized borided specimen exhibit two phase iron boride at the diffused zone with the formation of sawtooth morphology. The hardness gradient is gradually drops from borided zone to base metal. The 950°C 180minutes borided samples exhibits sudden drops of hardness gradient from surface to matrix. The content of FeB formation is lower than other higher temperature and long prolongation period conditions. The 950°C 180minutes boriding process exhibit grain coarsening effect in the transient zone. The depth of the continuous and optimum boride layer exhibit 96µm and 62µm respectively.

3.4. X-ray diffraction analysis

The XRD result revealed that the two phase iron borides were formed in both optimized boriding specimen and 950°C 180minutes borided specimen. In Optimized boriding, the formation of FeB phase is minimum and at the process of 950°C 180minutes boriding, the formation of FeB phase is maximum. The differences in FeB peak are attributable to process duration and temperature maintenance. The following figure of both the XRD processes are shown in Figure 5.

3.5. Hardness analysis

The hardness of optimized parameter exhibits $1680 \pm 15\text{HV}$ at the FeB zone then it reduces to 1425 ± 25 in the Fe₂B zone. Then the value of hardness is drops to $395 \pm 10\text{HV}$ in the transient zone. At last, $280 \pm 5\text{HV}$

Table 8: Validation result of pack boriding process.

SL.NO	RESPONSE	PREDICTED RESULTS	DESIRABILITY	EXPERIMENTAL RESULTS	ERROR (%)
1.	Microhardness	1649.1	0.989	1740	1.05
2.	Impact toughness	44.8	0.989	40	1.10

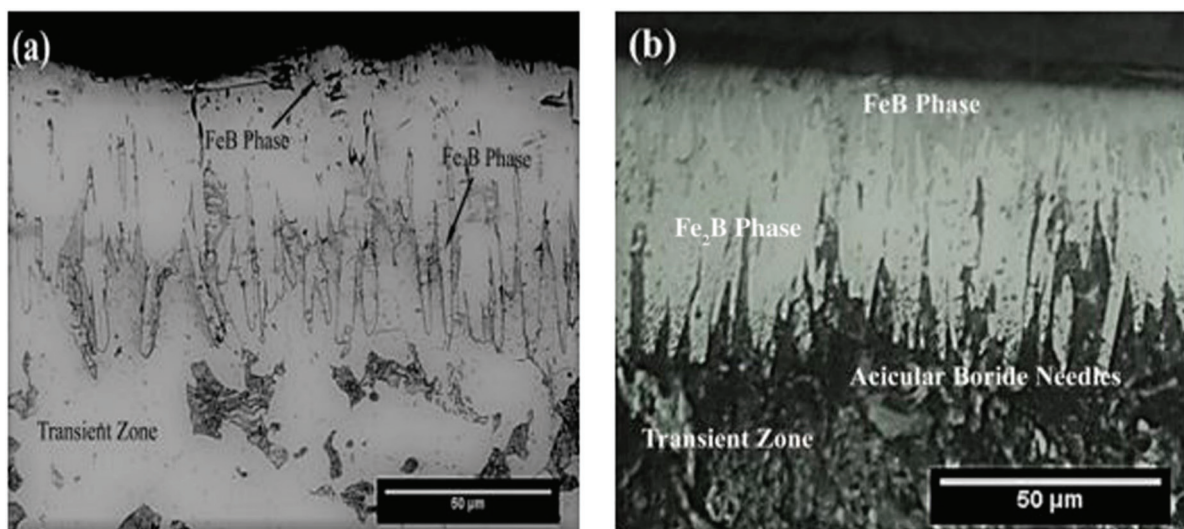


Figure 4: (a) Microstructure of pack borided at 850°C, 60minutes and (b) microstructure of pack borided at 950°C, 180minutes.

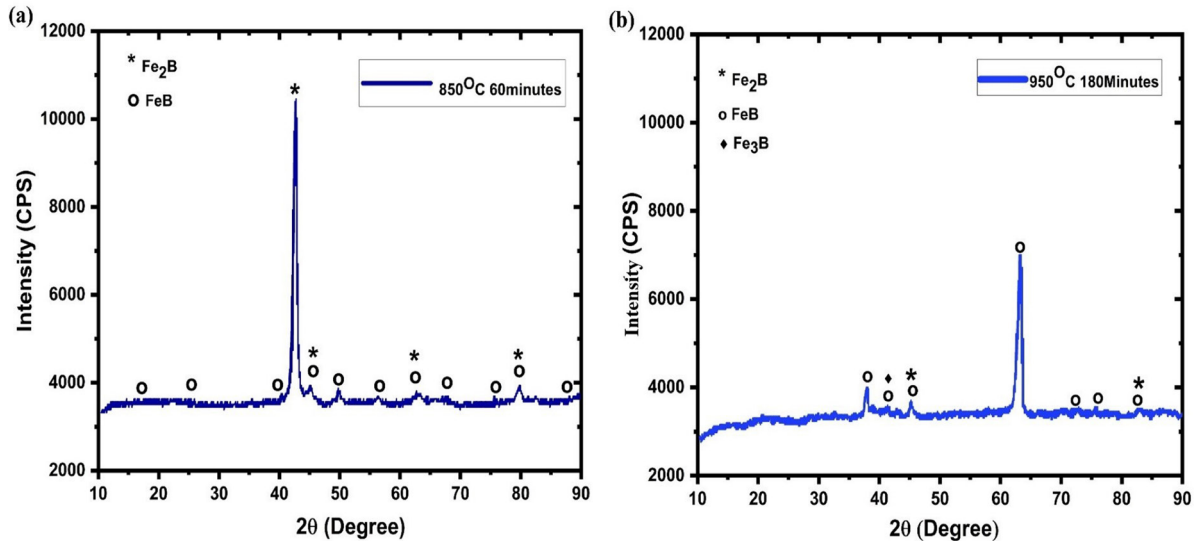


Figure 5: (a) XRD results of 850°C, 60minutes pack boriding process (b) XRD result of 950°C, 180minutes pack boriding process.

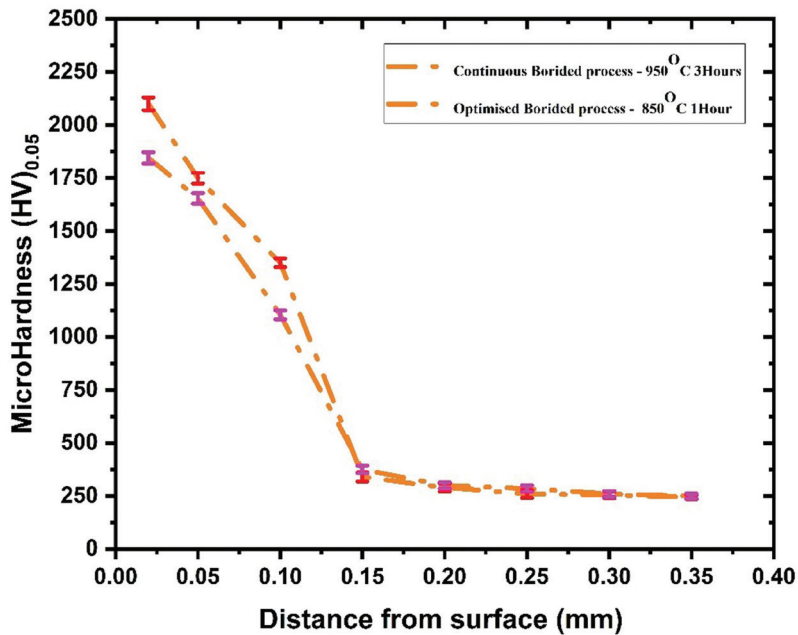


Figure 6: Comparison of microhardness analysis of specimens pack borided at 850°C, 60minutes and pack borided at 950°C, 180minutes.

was obtained in the zone of base metal. In the process of 950°C 180minutes borided sample, 2010 ± 25HV was obtained in FeB phase region. Then 1715 ± 20HV was obtained in the Fe₂B phase region. Then the value of hardness is suddenly drops to 315 ± 10HV in the transient zone. Finally, 265 ± 5HV was obtained in the matrix region. It indicates that the hardness gradient of optimized borided sample exhibits better value than 950°C 180minutes borided process. Process time and temperature both contribute to the enhancement of the hardness gradient. The graph of optimized boriding and 950°C 180minutes boriding is shown in Figure 6.

3.6. Impact test analysis

The impact test of optimized borided specimen exhibit better toughness value than 950°C 180minutes borided samples at the applied constant load condition. This is purely depending upon time, temperature, and chemical composition [33]. The value of toughness value of optimized boriding exhibit 40 J and the value of 950°C 180minutes boriding exhibit 12 J respectively. It confirms that optimized borided specimen exhibit 3.3 times

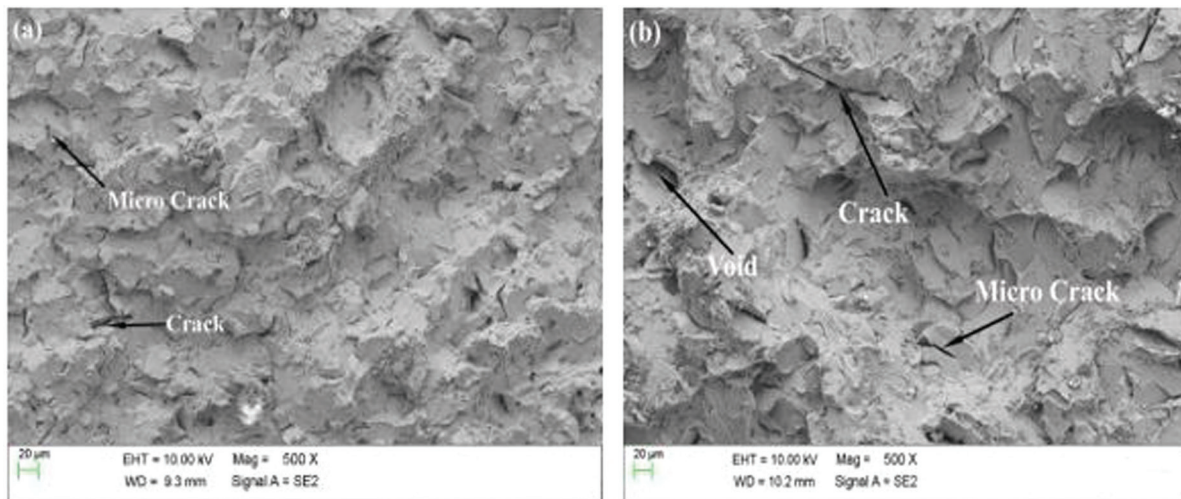


Figure 7: SEM images of specimens (a) pack borided at 850°C 60minutes and (b) pack borided at 950°C 180minutes.

higher toughness than 950°C 180minutes boriding. The SEM image of optimized boriding process and 950°C 180minutes boriding Processes are shown in Figure 7. The optimized borided method exhibits cleavage structures and numerous dimples in between them, indicating ductile – brittle fracture mode of failure [34]. Round pores and pits with fewer micro cracks were observed at the region. It is due to the diffusivity of boron elements is decreased due to the shorter process time and lower temperature. In the process of 950°C 3Hour boriding represent the formation of cleavage structure with the formation of secondary cracks. The formation of secondary cracks is due to the effect of high hardness of the material. This indicates the failure was occurred in the manner of brittle mode. Finally, it confirms that optimized borided process had an ability to increase toughness while concurrently decreasing brittleness.

4. CONCLUSION

The important results are summarized as follows:

- Using the RSM approach, empirical models for impact toughness and microhardness have been created. According to the regression models, temperature and time have the most impacts on impact toughness and microhardness. The values of microhardness and toughness are 1649.14HV_{0.5} and 44.8 J, respectively, are predicted under optimized conditions of 850°C 60minutes of processing time.
- Predicted and actual results are consistently correlated. The regression models capacity to predict outcomes is confirmed by the proof experiment. It has been determined that there is a 1.05% error for microhardness and a 1.10% error for impact toughness between anticipated and experimental results.
- The RSM models are effective for determining the optimized process parameters, which are then used to calculate the effective value for microhardness and impact toughness.
- The MCIBC borided sample exhibits three distinct zones in its microstructure: 1. Zone of iron boride (Fe₂B and FeB Phases) 2. The transition zone; 3. The base material.
- The optimum Boride layer's surface hardness at the material's surface is 1745HV_{0.5}. At the transition zone, the microhardness value drops to 345HV_{0.5}. At the base material, the hardness drops to 245HV_{0.5}. In the continuous boriding method, the boride layer's hardness was 2100HV_{0.5}, 375HV_{0.5} in the transient zone, and 215HV_{0.5} in the base metal. The hardness gradient quickly decreases from the surface of the boride layer to the base metal as compared to the optimized boriding procedure.
- The XRD results show that Fe₂B and FeB phases are present during both the optimized boriding method and the 950°C 180minutes boriding process. The growth of the FeB phase during the optimum 180minutes boriding procedure is less than 950°C.
- Compared to the 950°C 180minutes boriding technique, the impact toughness of the optimized boriding method was 3.3 times greater. The processing time, temperature, and behavior are responsible for this improvement. Continuous heating causes the treated steel to become more brittle in continuous boriding. It has the effect of decreasing toughness' value.

5. BIBLIOGRAPHY

- [1] MEDVEDOVSKI, E., ANTONOV, M., “Erosion studies of the iron boride coatings for protection of tubing components in oil production, mineral processing and engineering applications”, *Wear*, v. 452–453, pp. 203277, Jul. 2020. doi: <https://doi.org/10.1016/j.wear.2020.203277>
- [2] MISHIGDORZHIYN, U., CHEN, Y., ULAKHANOV, N., *et al.*, “Microstructure and wear behavior of tungsten hot-work steel after boriding and boroaluminizing”, *Lubricants*, v. 8, n. 3, pp. 26, Mar. 2020. doi: <https://doi.org/10.3390/lubricants8030026>
- [3] GUNEN, A., KANCA, Y., KARAHAN, I.H., *et al.*, “A comparative study on the effects of different thermochemical coating techniques on corrosion resistance of STKM-13A steel”, *Metallurgical and Materials Transactions. A, Physical Metallurgy and Materials Science*, v. 49, n. 11, pp. 5833–5847, Aug. 2018. doi: <http://dx.doi.org/10.1007/s11661-018-4862-2>
- [4] LÓPEZ PERRUSQUÍA, N., DOÑU RUIZ, M.A., GARCÍA BUSTOS, E.D., *et al.*, “Duplex surface treatment on microalloy steels by dehydrated paste pack boriding and pack carburizing”, *Materials Letters*, v. 280, n. 128573, pp. 1–5, Aug. 2020. doi: <http://dx.doi.org/10.1016/j.matlet.2020.128573>
- [5] GUNES, I., ERDOGAN, M., GÜRHAN, A., “Corrosion behavior and characterization of plasma nitrided and borided AISI M2 steel”, *Materials Research*, v. 17, n. 3, pp. 612–618, Mar. 2014. doi: <http://dx.doi.org/10.1590/S1516-14392014005000061>
- [6] ZENG, J., HU, J., YANG, X., *et al.*, “Evolution of the microstructure and properties of pre-boronized coatings during pack-cementation chromizing”, *Coatings*, v. 10, n. 2, pp. 159, Feb. 2020. doi: <http://dx.doi.org/10.3390/coatings10020159>
- [7] KAYALI, Y., KANCA, E., GUNEN, A., “Effect of boronizing on microstructure, high - temperature wear and corrosion behaviour of additive manufactured Inconel 718”, *Materials Characterization*, v. 191, pp. 112155, Sep. 2022. doi: <http://dx.doi.org/10.1016/j.matchar.2022.112155>
- [8] PRINCE, M., RAJ, G.S., KUMAR, D.Y., *et al.*, “Boriding of steels: improvement of mechanical properties — a review”, *High Temperature Material Processes*, v. 26, n. 2, pp. 43–89, May. 2020. doi: <http://dx.doi.org/10.1615/HighTempMatProc.2022041805>
- [9] CAMPOS-SILVA, I., FLORES-JIMÉNEZ, M., BRAVO-BÁRCENAS, D., *et al.*, “Evolution of boride layers during a diffusion annealing process”, *Surface and Coatings Technology*, v. 309, pp. 155–163, Nov. 2017. doi: <http://dx.doi.org/10.1016/j.surfcoat.2016.11.054>
- [10] TURKMEN, İ., YALAMAÇ, E., “Effect of alternative boronizing mixtures on boride layer and tribological behaviour of boronized SAE 1020 steel”, *Metals and Materials International*, v. 28, n. 5, pp. 1114–1128, Apr. 2020. doi: <http://dx.doi.org/10.1007/s12540-021-00987-8>
- [11] PRINCE, M., THANU, A.J., “The effects of boriding and heating on the ductility, strength, and toughness of AISI 1045 steel”, *High Temperature Material Processes*, v. 23, n. 2, pp. 107–120, 2019. doi: <http://dx.doi.org/10.1615/HighTempMatProc.2019030266>
- [12] KEDDAM, M., ORTIZ-DOMÍNGUEZ, M., SIMÓN-MARMOLEJO, I., *et al.*, “Pack-boriding of AISI P20 steel: estimation of boron diffusion coefficients in the Fe₂B layers and tribological behaviour”, *International Journal of Surface Science and Engineering*, v. 11, n. 6, pp. 563–585, Jan. 2020. doi: <http://dx.doi.org/10.1504/IJSURFSE.2017.088997>
- [13] FANG, H., XU, F., ZHANG, G., “Investigation of dry sliding wear behavior of pack boriding Fe-Based powder metallurgy”, *Integrated Ferroelectrics*, v. 208, n. 1, pp. 67–82, Jun. 2020. doi: <http://dx.doi.org/10.1080/10584587.2020.1728717>
- [14] NORA, R., ZINE, T.M., “Boriding and boronitrocarburising effects on hardness, wear and corrosion behavior of AISI 4130 steel”, *Revista Materia*, v. 24, n. 1, pp. e-12327, May. 2014. doi: <https://doi.org/10.1590/S1517-707620190001.0609>
- [15] HERNÁNDEZ-SÁNCHEZ, E., DOMÍNGUEZ-GALICIA, Y.M., OROZCO-ÁLVAREZ, C., *et al.*, “A study on the effect of the boron potential on the mechanical properties of the borided layers obtained by boron diffusion at the surface of AISI 316L steel”, *Advances in Materials Science and Engineering*, v. 2014, pp. 249174, 2014. doi: <http://dx.doi.org/10.1155/2014/249174>
- [16] GUNEN, A., ULUTAN, M., GOK, M.S., *et al.*, “Friction and wear behaviour of borided AISI 304 stainless steel with nano particle and micro particle size of boriding agents”, *Journal of the Balkan Tribological Association*, v. 20, n. 3, pp. 362–379, Jan. 2014.
- [17] GÜNEN, A., KANCA, E., DEMİR, M., *et al.*, “Microabrasion wear behavior of fast-borided steel tooth drill bits”, *Tribology Transactions*, v. 60, n. 2, pp. 267–275, Aug. 2017. doi: <http://dx.doi.org/10.1080/10402004.2016.1159359>

- [18] VANEGAS, L.G., ELÍAS ESPINOSA, M.C., PERRUSQUIA, N.L., *et al.*, “Analysis of the wear mechanisms of the boriding drill tip”, *Microscopy and Microanalysis*, v. 27, n. S1, pp. 3406–3408, Aug. 2021. doi: <http://dx.doi.org/10.1017/S1431927621011703>
- [19] MATHEW, M., RAJENDRAKUMAR, P.K., “Effect of precarburization on growth kinetics and mechanical properties of borided low-carbon steel”, *Materials and Manufacturing Processes*, v. 29, n. 9, pp. 1073–1084, Jul. 2014. doi: <http://dx.doi.org/10.1080/10426914.2014.901538>
- [20] ERDOGAN, A., “Boriding temperature effect on micro-abrasion wear resistance of borided tool steel”, *Journal of Tribology*, v. 141, n. 12, pp. 121702–121708, Sep. 2019. doi: <http://dx.doi.org/10.1115/1.4044859>
- [21] KRELLING, A.P., DA COSTA, C.E., MILAN, J.C.G., *et al.*, “Micro-abrasive wear mechanisms of borided AISI 1020 Steel”, *Tribology International*, v. 111, pp. 234–242, 2017. doi: <http://dx.doi.org/10.1016/j.triboint.2017.03.017>
- [22] GUNEN, A., MAKUCH, N., ALTINAY, Y., *et al.*, “Determination of fracture toughness of boride layer growth on $\text{Co}_{1.21}\text{Cr}_{1.82}\text{Fe}_{1.44}\text{Mn}_{1.32}\text{Ni}_{1.12}\text{Al}_{0.08}\text{B}_{0.01}$ high entropy alloy by nanoindentation”, *Ceramics International*, v. 48, n. 24, pp. 36410–36424, Dec. 2022. doi: <http://dx.doi.org/10.1016/j.ceramint.2022.08.201>
- [23] GUNEN, A., KURT, B., SOMUNKIRAN, I., *et al.*, “The effect of process conditions in heat - assisted boronizing treatment on the tensile and bending strength characteristics of the AISI - 304 austenitic stainless steel”, *The Physics of Metals and Metallography*, v. 116, n. 9, pp. 896–907, 2015. doi: <http://dx.doi.org/10.1134/S0031918X15090021>
- [24] KHURI, A.I., “A general overview of response surface methodology”, *Biometrics and Biostatistics International Journal*, v. 5, n. 3, pp. 87–93, Mar. 2017. doi: <http://dx.doi.org/10.15406/bbij.2017.05.00133>
- [25] MONTGOMERY, D.C., *Design and analysis of experiments*, New York, Wiley, pp. 1–688, 2009.
- [26] CAVDAR, F., GUNEN, A., KANCA, E., *et al.*, “An experimental and statistical analysis on dry sliding wear failure behaviour of Incoloy 825 at elevated temperatures”, *Journal of Materials Engineering and Performance*, v. 31, n. 9, pp. 4161–4184, Sep. 2022. doi: <https://doi.org/10.1007/s11665-022-07381-4>
- [27] TURKOGLU, T., AY, I., “Analysis of boride layer thickness of borided AISI 430 by response surface methodology”, *An International Journal of Optimization and Control: Theories and Applications*, v. 9, n. 3, pp. 39–44, 2019. doi: <http://dx.doi.org/10.11121/ijocta.01.2019.00660>
- [28] BABU, P.D., BUVANASHEKARAN, G., BALASUBRAMANIAN, K.R., “The elevated temperature wear analysis of laser surface-hardened EN25 steel using response surface methodology”, *Tribology Transactions*, v. 58, n. 4, pp. 602–615, May. 2015. doi: <http://dx.doi.org/10.1080/10402004.2014.998356>
- [29] ARGUELLES-OJEDA, J.L., “Hardness optimization of boride diffusion layer on ASTM F-75 alloy using response surface methodology”, *Revista Mexicana de Física*, v. 63, pp. 76–81, Feb. 2017.
- [30] SASHANK, S., BABU, P.D., MARIMUTHU, P., “Experimental studies of laser borided low alloy steel and optimization of parameters using response surface methodology”, *Surface and Coatings Technology*, v. 363, pp. 265–264, Apr. 2019. doi: <http://dx.doi.org/10.1016/j.surfcoat.2019.02.036>
- [31] ATUL, S.C., “Investigation on chromizing of C45 steel using response surface methodology”, *International Journal of Chemtech Research*, v. 9, n. 1, pp. 82–91, 2016.
- [32] ALAM, M.A., YA, H.H., AZEEM, M., *et al.*, “Modelling and optimisation of hardness behaviour of sintered Al/SiC composites using RSM and ANN: a comparative study”, *Journal of Materials Research and Technology*, v. 9, n. 6, pp. 14036–14050, Dec. 2020. doi: <http://dx.doi.org/10.1016/j.jmrt.2020.09.087>
- [33] PRINCE, M., ARJUN, S.L., SURYARAJ, G., *et al.*, “Experimental Investigations on the multicomponent laser boriding on steels”, *Materials Today: Proceedings*, v. 5, n. 11, pt 3, pp. 25276–25284, 2018. doi: <https://doi.org/10.1016/j.matpr.2018.10.330>
- [34] CAO, R., HAN, C., GUO, X., *et al.*, “Effects of boron on the microstructure and impact toughness of weathering steel weld metals and existing form of boron”, *Materials Science and Engineering A*, v. 833, pp. 142560, Jan. 2022. doi: <http://dx.doi.org/10.1016/j.msea.2021.142560>